International Journal of Pharmaceutics 383 (2010) 285–292

Contents lists available at ScienceDirect

International Journal of Pharmaceutics

journal homepage: www.elsevier.com/locate/ijpharm

Pharmaceutical Nanotechnology

Fabrication of drug nanoparticles by evaporative precipitation of nanosuspension

M. Kakran[a], N.G. Sahoo[a], L. Li[a,*], Z. Judeh[b], Y. Wang[c], K. Chong[d], L. Loh[d]

[a] School of Mechanical and Aerospace Engineering, Nanyang Technological University, 50 Nanyang Avenue, Singapore 639798, Singapore
[b] School of Chemical and Biomedical Engineering, Nanyang Technological University, 62 Nanyang Drive, Singapore 637459, Singapore
[c] Pharmacy Department, Inner Mongolia Medical College, Huhhot 010110, PR China
[d] Biomedical Engineering Group, School of Engineering (Manufacturing), Nanyang Polytechnic, 180 Ang Mo Kio Ave 8, Singapore 569830, Singapore

ARTICLE INFO

Article history:
Received 11 June 2009
Received in revised form
16 September 2009
Accepted 17 September 2009
Available online 23 September 2009

Keywords:
Malaria
Artemisinin
Crystallinity
Nanoparticles
Dissolution

ABSTRACT

Evaporative precipitation of nanosuspension (EPN) was used to fabricate nanoparticles of a poorly water-soluble antimalarial drug, artemisinin (ART), with the aim of enhancing its dissolution rate. We investigated the nanoparticle fabrication of ART via a full factorial experimental design considering the effects of drug concentration and solvent to antisolvent ratio on the physical, morphological and dissolution properties of ART. Characterization of the original ART powder and EPN prepared ART nanoparticles was carried out by scanning electron microscopy, differential scanning calorimetry (DSC), X-ray diffraction (XRD) and dissolution tester. DSC and XRD studies suggested that the crystallinity of EPN prepared ART nanoparticles decreased with increasing drug concentration and ratio of solvent to antisolvent. The particle diameters of EPN prepared ART nanoparticles were found to be 100–360 nm. The dissolution of EPN prepared ART nanoparticles markedly increased as compared to the original ART powder. A percent dissolution surface-response model was used to elucidate the significant and direct relationships between drug concentration and solvent to antisolvent ratio on one hand and percent dissolution on the other hand. The best dissolution percent was found to be 75.9%, at the drug concentration of 15 mg/mL and solvent to antisolvent ratio (by volume) of 1:20.

1. Introduction

The advanced drug discovery process today is leading to a vast number of drugs possessing a very good level of efficacy. Unfortunately, many of these drugs are exhibiting very poor water solubility (Lipinski et al., 2001). Poorly water-soluble drugs show a number of negative clinical effects like high local drug concentrations at the sites of the aggregate deposition, which could be associated with local toxic effects of the drug and its decreased systemic bioavailability (Yalkowsky, 1981). These drugs tend to be eliminated from the gastrointestinal tract before they get the opportunity to fully dissolve and be absorbed into the blood circulation. As about 65% of the human body is made up of water, a drug must be water-soluble and thus possess an acceptable bioavailability level. The great challenge in the pharmaceutical development is to create new formulation approaches and efficient drug-delivery systems to overcome solubility and dissolution problems of the drug candidates which are also often associated with poor oral bioavailability (Lipinski, 2002; Merisko-Liversidge, 2002).

The dissolution velocity and intestinal permeability are key determinants for the bioavailability, particularly for orally administered drugs. To evaluate and characterize pharmaceutical compounds with respect to their aqueous solubility and intestinal permeability, a biopharmaceutics classification system has been developed. The system divides drug compounds into four classes (Amidon et al., 1995). Class I drugs have high bioavailability and provide no challenge. Class IV drugs are pharmaceutical bricks which will never make them to the market. Class II and Class III drugs have a poor bioavailability because of their low solubility and their low membrane permeability, respectively. Drug candidates with successfully improved bioavailability by a solubilization technique belong to Class II, which means that their bioavailability is only limited by their poor aqueous solubility or dissolution velocity (Amidon et al., 1995).

Many approaches have been developed to enhance the dissolution velocity as well as bioavailability of poorly water-soluble drugs, including both modifications to the drug substance itself and the creation of specific formulations. Physical modifications to increase the surface area, solubility and wettability of the drug particles, therefore focus on particle size reduction (Subramaniam et al., 1997) or development of amorphous states (Hancock and Zografi, 1997; Grau et al., 2000). The most common method is to increase the surface area of the drug by micro/nano-nization. There are several methods for the size reduction of drug particles such as pulverization of large particles using a ball or jet mill, spray freezing, spray drying and supercritical antisolvent technique (SAS)

* Corresponding author. Tel.: +65 67906285; fax: +65 6791 1859.
E-mail address: mlli@ntu.edu.sg (L. Li).

0378-5173/$ – see front matter © 2009 Elsevier B.V. All rights reserved.
doi:10.1016/j.ijpharm.2009.09.030

(Billon et al., 2000; Jung and Perrut, 2001; Moretti et al., 2001; Hu et al., 2002; Rogers et al., 2002, 2003; Merisko-Liverside et al., 2003; Rasenack et al., 2003; Shariati and Peters, 2003; Dollo et al., 2004; Muhrer et al., 2006), etc. Particle size reduction by mechanical milling or high pressure homogenization has many limitations like often requiring long times, introducing impurities, and limiting flexibility in controlling particle size and morphology. Relative to mechanical micro/nano-nization process, precipitation from a solution can offer a greater flexibility for controlling the amorphous or crystalline form of a drug (Michal et al., 2006).

Artemisinin (ART) is a potent antimalarial drug that remains effective against multidrug resistant strains of Plasmodium falciparum malaria. It has good intestinal permeability and can readily cross the intestinal monolayers via passive diffusion (Augustijns et al., 1996). The major problem with artemisinin compounds is their poor aqueous solubility (Barradell and Fitton, 1995), resulting in poor absorption upon oral administration. This poor solubility, its short half life and high first-pass metabolism, might lead to incomplete clearance of the parasites resulting in recrudescence (Titulaer et al., 1991). Few studies investigated the enhancement of the dissolution of ART using a carrier like cyclodextrins (Wong and Yuen, 2001, 2003). They prepared cyclodextrin-ART complexes by using a slurry method at a molar ratio of 1:1 and showed that the β-cyclodextrin-ART complex has a faster rate and a higher extent of dissolution and possessed enhanced bioavailability *in vivo* compared with a commercial preparation containing the normal form of the drug.

In the present study, a method called evaporative precipitation of nanosuspension (EPN) has been developed and used to fabricate ART nanoparticles to enhance the dissolution rate of ART. The nanoparticles of ART were fabricated under various drug concentrations and ratios of solvent to antisolvent. Our experimental design allowed establishing a regression model that is used to understand the effects of the variables as well as to identify an optimal set of operational parameters for the best dissolution properties of the drug.

2. Materials and methods

2.1. Materials

Artemisinin was obtained from Kunming Pharmaceutical Corporation (Kunming, China). All the reagents used were of technical grade.

2.2. Method

ART nanoparticles were prepared by the EPN method. Original ART powder was dissolved in a good solvent (ethanol) and then nanosuspension was formed by quickly adding an antisolvent (hexane). Drug particles in the nanosuspension were obtained by quick evaporation of the solvent and antisolvent, followed by vacuum drying of the particles. The effects of parameters like drug concentration in solvent, and solvent to antisolvent ratio were investigated. The drug concentrations used were 5, 10, 15 mg/mL and the solvent to antisolvent (S-AS) ratios were varied to 1:10, 1:15, and 1:20 (by volume). Table 1 shows the samples prepared along with their preparation conditions.

2.3. Particle morphology

The morphology of samples was observed using a scanning electron microscope (JSM-6390LA-SEM, Jeol Co., Tokyo, Japan). The powder samples were spread on a SEM stud and sputtered with gold before the SEM observations. The analysis of the particle size was performed using the UTHSCSA *ImageTool* program.

2.4. DSC analysis

Differential scanning calorimetric (DSC) measurements were carried out using a PerkinElmer DSC 7 thermal analyzer in a temperature range of 50–250 °C at a heating rate of 10 °C/min in nitrogen gas. The melting point and heat of fusion were calculated using a DSC software.

2.5. X-ray diffraction analysis

X-ray diffraction was studied using the Bruker AXS D8 Advance X-ray diffractometer with Cu Kα—targets at a scanning rate of 0.010 2θ/s, 40 kV, 40 mA, to observe the crystallinity of samples.

2.6. Dissolution studies

The *in vitro* dissolution of the EPN prepared ART samples as well as the original ART powder were determined using the paddle method (USP apparatus II) (Verkin Dissolution Tester DIS 8000) in 900 mL of distilled water, under nonsink conditions. The paddle rotation was set at 200 rpm. The temperature was maintained at 37 ± 0.5 °C. 360 mg of the EPN prepared ART samples and original ART powder were used for the dissolution. Samples of 1 mL volume were collected at 0.5-, 1-, 2-, 3- and 4-h intervals.

2.7. Analysis of ART concentrations

The ART concentrations for the dissolution studies were determined using a high performance liquid chromatography (HPLC) method with ultraviolet detection (Zhao, 1987). The HPLC used was Agilent 1100 series, which was comprised of a degasser, a pump, an auto liquid sampler, a UV detector and a HPLC column. The column used was Kromasil C18 (150 mm × 4.6 mm id × 3.5 μm) (Eka Chemicals AB, Sweden). The mobile phase consisting of 75% of 0.01 M disodium hydrogen phosphate and 25% acetonitrile (HPLC grade)

Table 1
Different samples prepared according to the experimental design showing the scaled and the original variable values in bracket, and their observed and predicted percent dissolution at 4 h.

Sample	Drug concentration (mg/mL), X_1	Solvent to antisolvent ratio, X_2	Percent dissolution (observed) (%)	Percent dissolution (predicted) (%)
Original ART	–	–	13.10	–
No. 1	−1 (5)	−1 (1:10)	22.48	24.22 ± 4.81
No. 2	−1 (5)	0 (1:15)	21.20	20.27 ± 3.85
No. 3	−1 (5)	1 (1:20)	26.88	26.05 ± 4.81
No. 4	0 (10)	−1 (1:10)	14.15	14.52 ± 3.85
No. 5	0 (10)	0 (1:15)	15.10	15.14 ± 2.77
No. 6	0 (10)	1 (1:20)	30.99	33.49 ± 3.85
No. 7	1 (15)	−1 (1:10)	21.25	22.13 ± 4.81
No. 8	1 (15)	0 (1:15)	42.53	43.32 ± 3.85
No. 9	1 (15)	1 (1:20)	75.93	74.24 ± 4.81

was adjusted to pH 6.5 with glacial acetic acid. The flow rate was set at 0.8 mL/min. The detector was operated at a wavelength of 254 nm.

The samples were filtered through 0.45 μm polypropylene-reinforced Teflon membrane with polypropylene housing (Ministart-SRP 15, Saritorius, Germany). The samples were subjected to pretreatment prior to injection into the HPLC system. 1 mL of sample was added into 200 μL of 10 M sodium hydroxide and the mixture was heated at 45 °C for 25 min, which was then cooled to room temperature. Finally, 150 μL of glacial acetic acid was added into the above mixture before injection into the HPLC system.

2.8. Dissolution rate constant studies

The Noyes–Whitney equation is considered as a general guideline for how the dissolution rate of an insoluble drug might improve (Noyes and Whitney, 1897). The dissolution rate equation based on mass is expressed as follows:

$$\frac{dm}{dt} = K(M_S - m) \quad (1)$$

where m is the dissolution amount of drug at time t, dm/dt is the dissolution rate, M_S is the dissolution amount at infinite time, and t is the dissolution time. Integrating Eq. (1) with the initial condition of $m = 0$ for $t = 0$, then Eq. (2) is obtained.

$$m = M_S[1 - \exp(-Kt)] \quad (2)$$

Diving both sides by M_S, we get Eq. (3):

$$\frac{m}{M_S} = [1 - \exp(-Kt)] \quad (3)$$

where the dissolution rate constant K is defined as AD/h, where A is the surface area available for dissolution, D is the diffusion coefficient of the drug, and h is the thickness of the diffusion boundary layer adjacent to the surface of the dissolving drug.

3. Results and discussion

3.1. Experimental design and surface modeling

We have considered two process variables: drug concentration and solvent to antisolvent ratio. These two variables are independent of each other and controlled in the experiments. Statistical experimental design is used in this investigation to map the system and thus to approximate the percent dissolution (after 4 h) by a quadratic model. Such a model will allow us to (a) analyze and understand in more detail how the two variables influence the dissolution of fabricated particles, (b) make predictions of percent dissolution under different experimental conditions, (c) optimize the experimental conditions for maximum dissolution and thus (d) find an optimal range of experimental conditions. A full factorial Central Composite Face centered (CCF) experimental design was used to generate 11 runs. For the purpose of fitting the model, a design matrix is generated by centering and orthogonally scaling the original factor values according to:

$$z_i = \frac{X_i - M}{R}, \quad i = 1, 2, \ldots, k \quad (4)$$

where z denotes the scaled factor value, X is the original one, and M is the midrange while R is equivalent to half range. The range and level of factors used are displayed in coded units in Table 2. Original ART powder was dissolved in ethanol (solvent) at different drug concentrations from 5 to 15 mg/mL. Hexane (antisolvent) was added to the solution at different solvent to antisolvent ratios of 1:10–1:20 to obtain the nanosuspension, which was rapidly evaporated to obtain drug nanoparticles.

Table 2
The range of the two independent variables (factors) and the level of variables used in the experimental design.

Variable	Unit	Range	Design levels		
			−1	0	1
Drug concentration (X_1)	mg/mL	5–15	5	10	15
Solvent to antisolvent ratio (SAS) (X_2)	–	10–20	1:10	1:15	1:20

In the surface-response modeling exercise of this study, only one response to be considered is the percent dissolution (after 4 h). A Multilinear Regression Model (MLR) was fitted to the data considering the two independent variables (X_1 and X_2) and the one dependent response (Y). The resulting MLR model after eliminating insignificant terms is given by:

$$Y = \beta_0 + \beta_1 X_1 + \beta_2 X_2 + \beta_3 X_1^2 + \beta_4 X_2^2 + \beta_5 X_1 X_2 \quad (5)$$

The coefficients β of the regression model (Eq. (5)) calculated are listed in Table 3, in which they contain two linear, two quadratic and one interaction terms and one constant term. The p-values in Table 3 provide a check on the significance of each of the coefficients where a coefficient with a smaller p-value is more significant. This reveals the significance of the linear coefficient of the drug concentration term X_1 and solvent to antisolvent ratio term X_2; the quadratic coefficient of drug concentration term X_1^2; and interaction coefficient term X_1X_2. This suggests that drug concentration and solvent to antisolvent ratio and their interaction have a direct relationship with the percent dissolution of the fabricated drug particles. The Analysis Of Variance (ANOVA) test results are also shown in Table 3, indicating the goodness of the model as the value of the standard deviation of the regression (26.302) is much larger than the standard deviation of the residuals (2.099) with its upper confidence level of 95%. From the ANOVA test the model is also found to be highly significant as the F-value (156.994) is very high compared to the upper critical value (4.619) of the F-value ($F_{15,5}$) at the 5% significance level.

The model predictions under the conditions of the experiments given in the experimental design are listed in Table 1 along with their corresponding uncertainties. An 'observed versus predicted' plot is shown in Fig. 1. From this parity plot, the correlation coefficient of the model was determined to be $R^2 = 0.9957$, indicating that the model is suitable for representing the factor–response relationships within the variable ranges studied. The model can now be used for understanding the relationships between the factors and the percent dissolution of the products. Fig. 2(i) and (ii) shows the prediction plots of percent dissolution against each of the studied factors.

The model was also used in an optimization exercise, identifying the optimal experimental conditions within the variable ranges

Table 3
Calculated coefficient values and ANOVA.

Model term	Coefficient	Value	SE	p-value
Constant	β_0	15.142	1.077	0.0000
X_1	β_1	11.525	0.857	0.0000
X_2	β_2	13.485	0.857	0.0000
X_1^2	β_3	16.658	1.319	0.0000
X_2^2	β_4	4.863	1.319	0.0142
$X_1 X_2$	β_5	12.569	1.050	0.0000

ANOVA

	df	SS	MS	SD	F-value	p-value
Total corrected	10	3481.050	348.105	18.658	156.994	0.000
Regression	5	3459.020	691.804	26.302		
Residual	5	22.033	4.407	2.099		

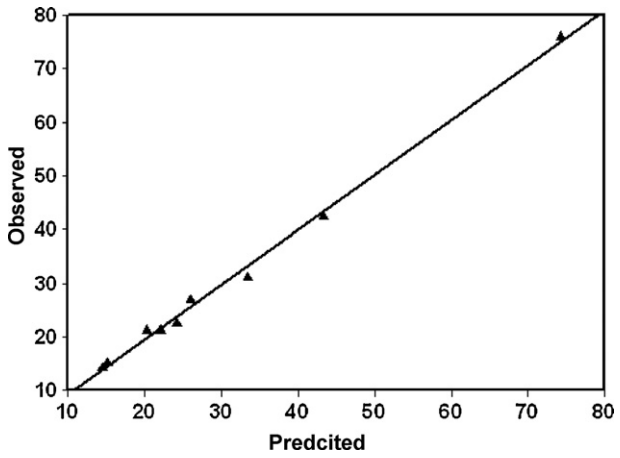

Fig. 1. Observed versus predicted percent dissolution with $r^2 = 0.9957$.

studied as: drug concentration of 15 mg/mL, and solvent to antisolvent ratio of 1:20. The optimal percent dissolution (after 4 h) was calculated to be at a high value of 74.24 ± 4.81%. The regression and statistical analyses were carried out using MODDE (Umetrics, Umeå, Sweden). The Optimizer function within MODDE was used to carry out the optimization of the experimental variables for a maximum percent dissolution criteria.

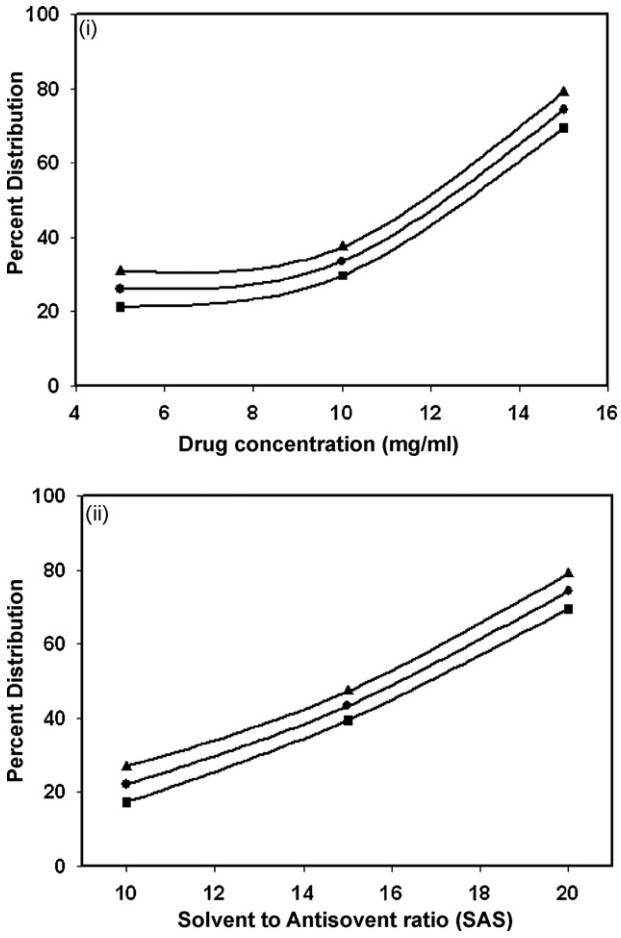

Fig. 2. (i) Predicted percent dissolution versus drug concentration at the identified optimal condition of solvent to antisolvent ratio = 20. (●) Percent dissolution, (■) lower confidence interval, and (▲) upper confidence interval. (ii) Predicted percent dissolution versus solvent to antisolvent ratio at the identified optimal condition of drug concentration = 15 mg/mL. (●) Percent dissolution, (■) lower confidence interval, and (▲) upper confidence interval.

3.2. Particle morphology

We examined the effects of drug concentration and solvent to antisolvent ratio on preparing ART nanoparticles by the EPN process. SEM microphotographs of the original ART powder and EPN prepared ART particles under variable conditions are shown in Fig. 3. For the SEM study we have selected the samples to show the effects of drug concentration and solvent to antisolvent ratio on morphology of EPN prepared drug particles. It is observed from Fig. 5 that in the case of EPN prepared ART particles the diameters were in the range of 100–360 nm and the particles showed the needle type morphology. The original ART powder exhibited particles lacking uniformity in size and were much larger (5–50 μm) than the EPN prepared ones and had the different morphology. The EPN prepared nanoparticles were more uniform and the uniformity was more prominent at the higher solvent to antisolvent ratio. The size of the EPN prepared ART nanoparticles tended to decrease at high drug concentration and high solvent to antisolvent ratio. This observation can be interpreted by the formation of nanoparticles by homogeneous nucleation.

The rate of nucleation per unit volume and per unit time, R_N, is given by (Guozhong, 2003):

$$R_N = \left\{ \frac{C_0 kT}{3\pi\lambda^3 \eta} \right\} \exp\left(-\frac{\Delta G^*}{kT} \right) \quad (6)$$

where C_0 is the initial concentration, k is the Boltzmann constant, T is the temperature, λ is the diameter of the growth species, η is the viscosity of the solution and ΔG^* is the energy barrier that a nucleation process must overcome.

This equation indicates that high initial concentration or supersaturation (so, a large number of nucleation sites), low viscosity and low critical energy barrier favor the formation of a large number of nuclei. A larger number of nuclei mean smaller sized nuclei.

Once nuclei are formed, they grow simultaneously. For the synthesis of nanoparticles with a uniform size distribution, it is the best if all nuclei are formed at the same time. So it is highly desirable to have nucleation occur within a very short period of time. In our fabrication process, to achieve a sharp nucleation, the concentration of the growth species is increased abruptly to a very high supersaturation and then quickly brought below the minimum concentration for nucleation by quickly adding a higher ratio of antisolvent. Below this concentration, no more new nuclei are formed, whereas the existing nuclei continue to grow until the concentration of the growth species decreases to the equilibrium concentration. For the subsequent growth a high solvent to antisolvent ratio increases the diffusion distance for growth species and consequently diffusion becomes the limiting step for nuclei growth (Guozhong, 2003).

3.3. DSC analysis

In order to understand the effect of the evaporative precipitation of nanosuspension process on the thermal properties of ART, DSC was conducted. DSC thermograms of original ART powder is compared to the various samples prepared in Fig. 4. The heat of fusion (ΔH_f) obtained from the DSC study is summarized in Table 4. The original ART powder used in this study had a sharp melting endothermic peak at 156 °C. The endothermic melting peaks of the samples prepared by EPN were almost similar to the original ART powder. However, the heat of fusion of the original ART powder was higher than that of the EPN prepared ART particles. The heat of fusion of the EPN prepared samples depended on the drug concentration and the solvent to antisolvent ratio. At a constant drug concentration, the heat of fusion decreased with increasing solvent to antisolvent ratio as shown in the Fig. 4(i). The heat of fusion

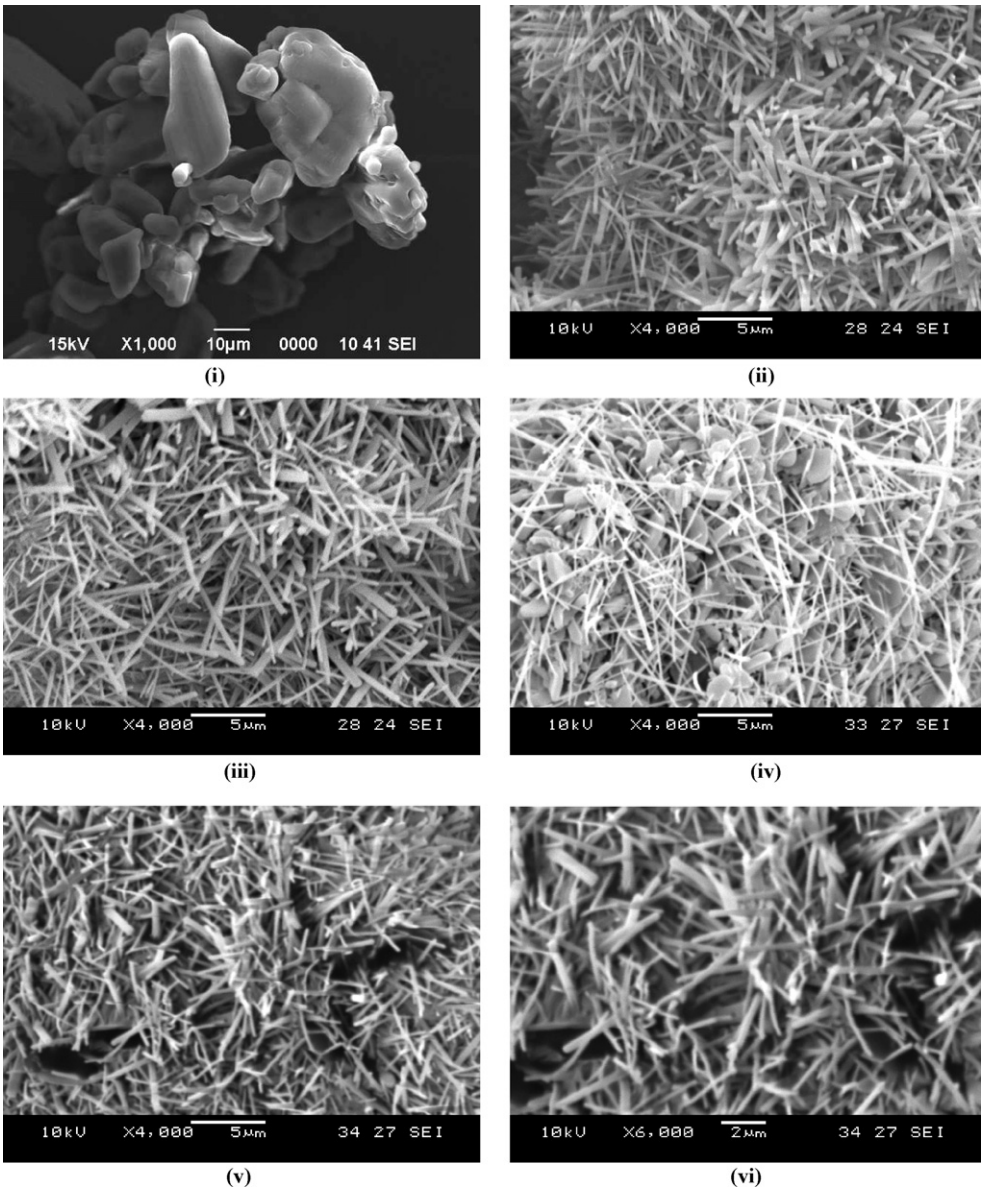

Fig. 3. SEM microphotographs of the original ART powder and EPN prepared ART particles, (i) original ART powder, (ii) EPN prepared No. 3, (iii) EPN prepared No. 6, (iv) EPN prepared No. 7, (v) EPN prepared No. 9, and (vi) higher magnification EPN prepared No. 9.

also decreased with increasing drug concentration at a particular solvent to antisolvent ratio as seen from Fig. 4(ii). Heat of fusion is proportional to the amount of crystallinity in the samples. These results suggest that the crystallinity of ART particles was decreased when the particles are prepared by EPN process, which was also supported by XRD analysis. Therefore, it appears that a reduction in crystallinity was achieved by EPN.

3.4. XRD analysis

The representative X-ray diffraction patterns of the original ART powder and EPN prepared samples are shown in Fig. 5. The figures indicated the changes in the drug crystal structure. The X-ray patterns of the original ART powder displayed the presence of numerous distinct peaks at 2θ of 7.29°, 11.78°, 14.65°, 15.63°, 16.64°, 18.23°, 20.0°, and 22.1°, which suggested the that drug was of crystalline form. The EPN prepared samples showed the similar diffraction pattern but with lower peak intensity, suggesting the crystallinity of EPN prepared ART particles decreased during the EPN process. It is very interesting to note that a new diffraction peak appeared at $2\theta = 9.24°$ for the most of the EPN prepared samples. These results suggest a change in the crystal structure of ART.

The prominent peaks of EPN prepared ART samples were influenced by the drug concentration and the solvent to antisolvent ratio. At a constant drug concentration, the diffraction peak intensity decreased as the solvent to antisolvent ratio increased as shown in Fig. 5. The diffraction peak intensity was also decreased at the higher drug concentration and at high solvent to antisolvent ratio. From XRD observations, we can conclude that the crystalline nature of the drug was still maintained, but the relative reduction of diffraction intensity of ART in the EPN prepared samples suggests that the quality of crystals was reduced.

3.5. Dissolution studies

Table 4 shows the experimental data for the dissolution of the original ART powder and the EPN prepared ART particles. Fig. 6

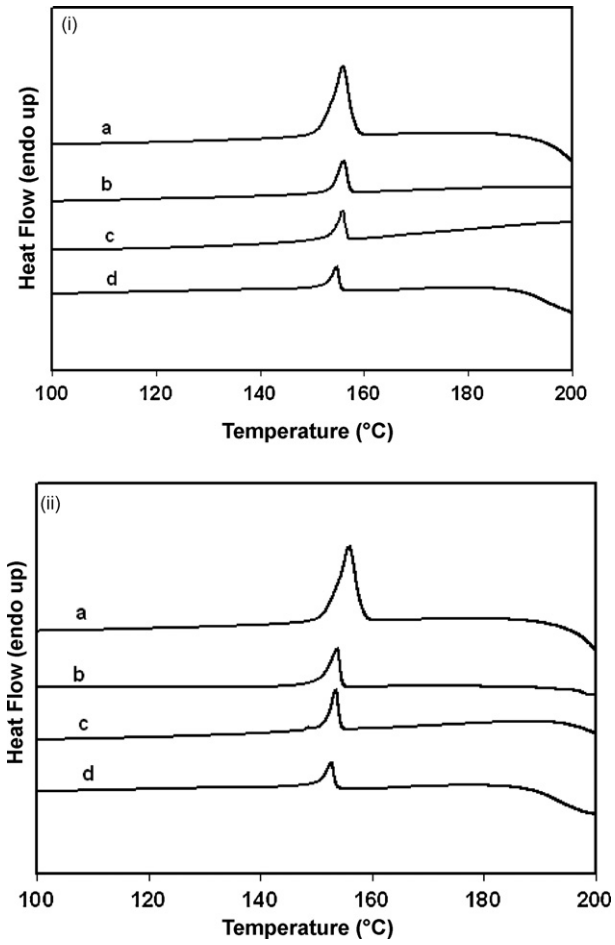

Fig. 4. (i) DSC thermograms showing the varying solvent to antisolvent ratios (1:10, 1:15, 1:20) for the drug concentrations 15 mg/mL. (a) original ART powder, (b) EPN ART No. 7, (c) EPN ART No. 8, and (d) EPN ART No. 9. (ii). DSC thermograms showing the varying drug concentrations (5, 10, 15 mg/mL) for the solvent to antisolvent ratio 1:20. (a) Original ART powder, (b) EPN ART No. 3, (c) EPN ART No. 6, and (d) EPN ART No. 9.

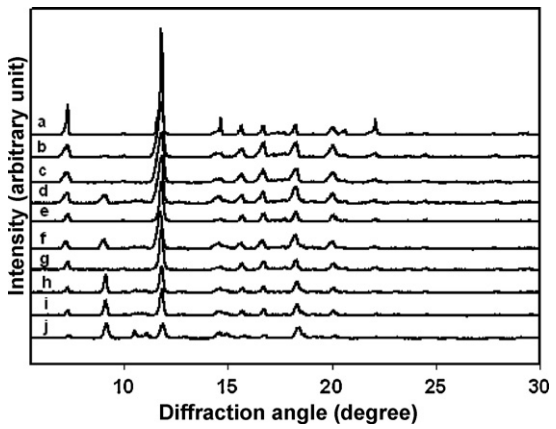

Fig. 5. X-ray diffractograms of the original ART powder and EPN prepared ART particles, (a) original ART powder, (b) No. 1, (c) No. 2, (d) No. 3, (e) No. 4, (f) No. 5, (g) No. 6, (h) No. 7, (i) No. 8, and (j) No. 9.

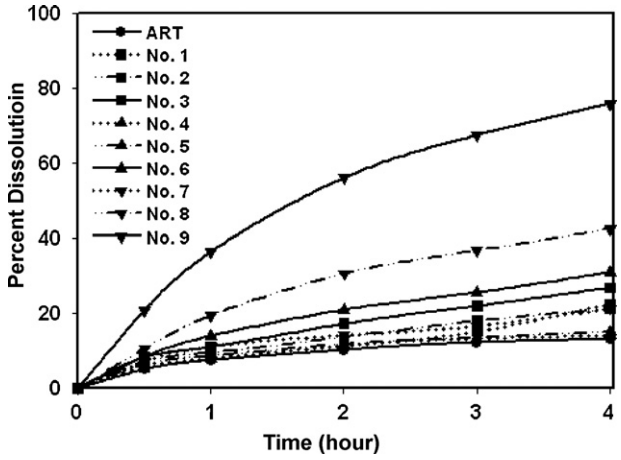

Fig. 6. Dissolution profile of original ART powder and all EPN prepared samples.

shows the dissolution profiles for original ART powder and the EPN prepared ART samples. The dissolution of the original ART powder in water was very low as seen from the experimental data that after 4 h only about 13.1% of the original ART powder was dissolved. For the EPN prepared samples the dissolution rate was better, the best was No. 9, where 75.9% drug was dissolved after 4 h. This result implied the approximately 5.8 times substantial increase in the percent dissolution from the original ART. For the original ART the actual amount dissolved after 4 h was 52.40 μg/mL, whereas for the EPN prepared sample No. 9 the actual amount dissolved after 4 h was 303.72 μg/mL. Comparing with enhancement of the dissolution of ART using carrier like cyclodextrins prepared by the slurry method, the maximum amount dissolved for ART–β-cyclodextrin complex was around 120 μg/mL, corresponding to about 43.2% dissolution after 8 h (Wong and Yuen, 2001, 2003).

It can be seen from Fig. 7 that during the EPN process as the drug concentration increased the effect of solvent to antisolvent ratio effect on the dissolution of ART became more and more prominent. At the lower drug concentration (5 mg/mL), increasing the solvent to antisolvent ratio from 1:10 to 1:20 increased the percent dissolution from 22.5% to only 26.9%, whereas at the higher drug concentration (15 mg/mL), the percent dissolution increased from

Table 4
Experimental data of percent dissolution, dissolution rate constant (K) and heat of fusion (ΔH_f) for original ART and EPN prepared samples.

Sample	Dissolution percent						Dissolution rate constant, K	ΔH_f (J/g)
	$t=0$	$t=0.5$	$t=1$	$t=2$	$t=3$	$t=4$		
Original ART	0	5.00	7.50	10.28	12.21	13.10	0.0428	76.20
No. 1	0	5.45	8.10	11.21	15.13	22.48	0.0617	71.98
No. 2	0	7.10	9.52	13.65	17.98	21.20	0.0665	72.64
No. 3	0	8.25	10.98	17.25	21.95	26.88	0.0853	70.39
No. 4	0	6.05	7.76	11.45	13.21	14.15	0.0468	74.18
No. 5	0	6.4	8.65	11.78	13.54	15.10	0.0494	74.18
No. 6	0	8.43	13.98	20.97	25.56	30.99	0.1028	69.39
No. 7	0	7.05	11.18	14.12	16.60	21.25	0.0662	72.35
No. 8	0	10.60	19.45	30.65	36.79	42.53	0.1577	67.12
No. 9	0	20.85	36.50	56.23	67.58	75.93	0.3975	59.18

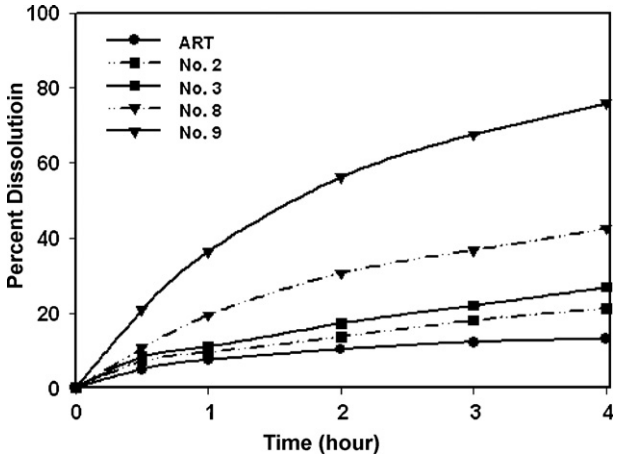

Fig. 7. Dissolution profile of original ART powder and EPN prepared samples showing the effect of varying solvent to antisolvent ratios (1:15 and 1:20) for the 2 drug concentrations (5 and 15 mg/mL).

21.3% to a high of 75.9% by increasing the solvent to antisolvent ratio from 1:10 to 1:20. Another observation from Fig. 7 was that at a low solvent to antisolvent ratio (1:10), drug concentration did not have significant effect on the percent dissolution of ART. This was because at a low solvent to antisolvent ratio, the diffusion distance for growth species was reduced and thus nuclei growth became more dominant and thus, increased particle size. So, even if there was higher nucleation due to higher concentration, the particle size still increased due to nuclei growth as a result of low solvent to antisolvent ratio. But at higher solvent to antisolvent ratio, the effect of drug concentration on percent dissolution was enhanced with the drug concentration.

From the Noyes–Whitney equation, the values of dissolution rate constant K for the original ART powder and the EPN prepared samples were obtained according to the Eq. (3). The calculated values of dissolution rate constant K, along with ΔH_f is listed in Table 4. Fig. 8 shows the experimental data as well as the data obtained from the model for the original ART and for EPN prepared sample No. 9. The Pearson product–moment correlation coefficient (PMCC, and typically denoted by r), a common measure of the correlation between two variables was used to find the correlation between the experimental values and the values obtained from the model for both original ART and the EPN prepared sample No. 9. The correlation coefficient between experimental values and the values obtained from the model for ART (r_{ART}) was calculated to be 0.9379,

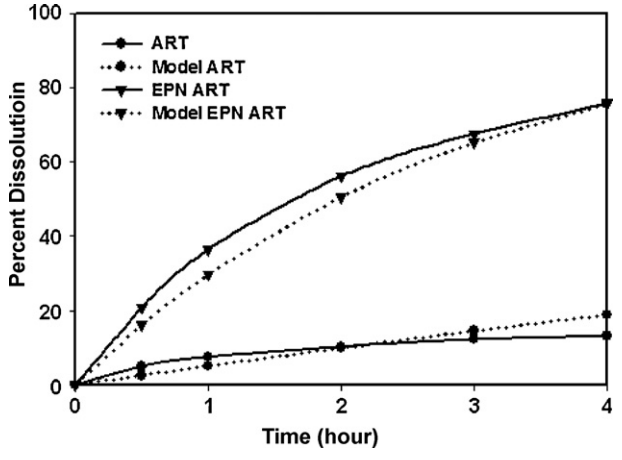

Fig. 8. Comparison of the experimental and the data obtained from the model for original ART powder and for EPN prepared sample No. 9.

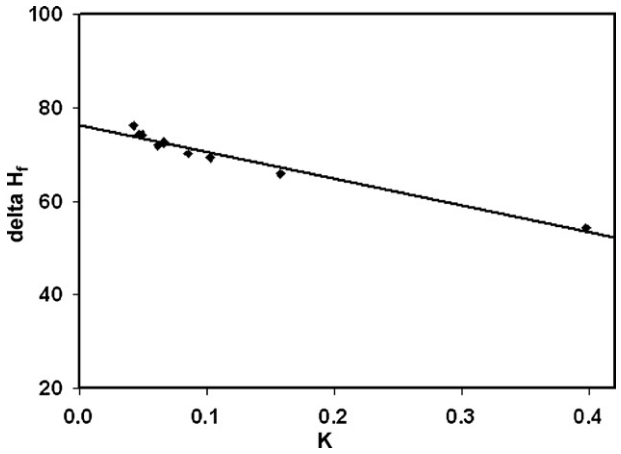

Fig. 9. Correlation between ΔH_f and dissolution rate constant K for ART drug particles with $r^2 = 0.9662$.

which was considered as a strong correlation. The correlation coefficient between the experimental values and the values obtained from the model for the EPN prepared sample No. 9 ($r_{EPN\,9}$) was calculated to be 0.9971, which was considered as a very strong correlation. Hence, the model and value of K were highly correlated with the experimental data obtained. The correlation between the enthalpy of fusion ΔH_f and the dissolution rate constant K was also examined. Fig. 9 shows the correlation between ΔH_f and the dissolution rate constant K. As shown in the Fig. 9, K increased with decreasing ΔH_f with good linearity as shown by the r^2 value of 0.9662 in the figure. DSC and XRD studies revealed that the crystallinity of the EPN prepared ART nanoparticles was lower at high drug concentration and high solvent to antisolvent ratio, which increased the percent dissolution.

According to the Noyes–Whitney equation, the dissolution rate of drug can be increased by reducing the particle size to increase the particles surface area. The particle size of the original ART powder was reduced from a size range of approximately 5–50 μm to around 100–360 nm by EPN, which increased the percent dissolution for the EPN prepared drug nanoparticles. The extent of crystallinity also influences the dissolution rate of the drug. An amorphous or metastable form dissolves at a faster rate because of its higher internal energy and greater molecular motion, which enhances the thermodynamic properties compared to crystalline materials. Our EPN prepared drug nanoparticles exhibited lower crystallinity compared to the original ART, and hence showed enhanced dissolution. We found that the percent dissolution of the EPN prepared samples depended on the drug concentration and the solvent to antisolvent ratio. This dependency was analyzed, using the identified model, at the identified optimal conditions (drug concentration = 15 mg/mL, solvent to antisolvent ratio = 1:20). The results of this analysis are displayed in Fig. 2(i) and (ii) showing that at the optimal conditions the percent dissolution of the EPN prepared drug particles increased with increasing drug concentration and solvent to antisolvent ratio. Our EPN prepared ART had the higher dissolution rate, which could translate into increased bioavailability upon oral administration.

4. Conclusions

This study demonstrated that the EPN method is able to prepare ART nanoparticles with significantly higher percent dissolution in water. The method developed is very cost effective, easy to operate and can be easily scaled for industrial production of drug nanoparticles. The percent dissolution of ART nanoparticles depended

on particle size, crystallinity, drug concentration, and solvent to antisolvent ratio. ART nanoparticles produced by our fabrication method would have high potential for delivery in much smaller doses compared with commercial preparation containing the normal form of the drug.

Acknowledgements

Authors acknowledge the financial support from Lee Kuan Yew Post Doctoral Fellowship, Nanyang Technological University, Singapore.

References

Amidon, G.L., Lennernas, H., Shah, V.P., Crison, J.R., 1995. A theoretical basis for a biopharmaceutic drug classification: the correlation of in vitro drug product dissolution and in vivo bioavailability. Pharm. Res. 12, 413–420.

Augustijns, P., D'Hulst, A., Daele, J.V., Kinget, R., 1996. Transport of artemisinin and sodium arsenate in caco-2 intestinal epithelial cells. J. Pharm. Sci. 85, 577–579.

Barradell, L.B., Fitton, A., 1995. Artesunate. A review of its pharmacology and therapeutic efficacy in the treatment of malaria. Drugs 50, 714–741.

Billon, A., Bataille, B., Cassanas, G., Jacob, M., 2000. Development of spray-dried acetaminophen microparticles using experimental designs. Int. J. Pharm. 203, 159–168.

Dollo, G., Le Corre, P., Guerin, A., Chevanne, F., Burgot, J.L., Leverge, R., 2004. Spray-dried redispersible oil-in-water emulsion to improve oral bioavailability of poorly soluble drugs. Eur. J. Pharm. Biopharm. 19, 273–280.

Grau, M.J., Kayser, O., Muller, R.H., 2000. Nanosuspensions of poorly soluble drugs-reproducibility of small scale production. Int. J. Pharm. 196, 155–157.

Guozhong, C., 2003. Nanostructures & Nanomaterials: Synthesis Properties & Applications. Imperial College Press, London, pp. 53–62.

Hancock, B.C., Zografi, G., 1997. Characteristics and significance of the amorphous state in pharmaceutical systems. J. Pharm. Sci. 86, 1–12.

Hu, J., Rogers, T.L., Brown, J.N., Young, T.J., Johnston, K.P., Williams, R.O., 2002. Improvement of dissolution rates of poorly water soluble APIs using the novel spray freezing into liquid technology. Pharm. Res. 19, 1278–1284.

Jung, J., Perrut, M., 2001. Particle design using supercritical fluids: literature and patent survey. J. Super Fluids 20, 179–219.

Lipinski, C., 2002. Poor aqueous solubility—an industry wide problem in drug delivery. Am. Pharm. Rev. 5, 82–85.

Lipinski, C.A., Lombardo, F., Dominy, B.W., Feeney, P.J., 2001. Experimental and computational approaches to estimate solubility and permeability in drug discovery and development settings. Adv. Drug Deliv. Rev. 46, 3–26.

Merisko-Liverside, E., Liversidge, G.G., Cooper, E.R., 2003. Nonosizing: a formulation approach for poorly-water soluble compounds. Eur. J. Pharm. Sci. 18, 113–120.

Merisko-Liversidge, E., 2002. Nanocrystals: Resolving Pharmaceutical Formulation Issues Associated with Poorly Water-soluble Compounds in Particles. Marcel Dekker, Orlando.

Michal, E., Matteucci, Margaret, A., Hotze, Keith, P., Johnston, Robert, O., Williams, 2006. Drug nanoparticles by antisolvent precipitation: mixing energy versus surfactant stabilization. Langmuir 22, 8951–8959.

Moretti, M.D.L., Gavini, E., Juliano, C., Pirisino, G., Giunchedi, P., 2001. Spray-dried microspheres coantaining ketoprofen formulated into capsules and tablets. J. Microencapsul. 18, 111–121.

Muhrer, G., Meier, U., Fusaro, F., Albano, S., Mazzotti, M., 2006. Use of compressed gas precipitation to enhance the dissolution behavior of a poorly water soluble drug: generation of drug microparticles and drug-polymer dispersions. Int. J. Pharm. 308, 69–83.

Noyes, A.A., Whitney, W.R., 1897. The rate of solution of solid substances in their own solutions. J. Am. Chem. Soc. 19, 930–934.

Rasenack, N., Hartenhauer, H., Muller, B.W., 2003. Microcrystals for dissolution rate enhancement of poorly water-soluble drugs. Int. J. Pharm. 254, 137–145.

Rogers, T.L., Hu, J., Yu, Z., Johnston, K.P., Williams, R.O., 2002. A novel particle engineering technology: spray-freezing into liquid. Int. J. Pharm. 242, 93–100.

Rogers, T.L., Overhoff, K.A., Shah, P., Santiago, P., Yacaman, M.J., Johnson, K.P., William III, R.O., 2003. Micronized powders of a poorly water soluble drug produced by a spray-feezing into liquid-emulsion process. Eur. J. Pharm. Biopharm. 55, 161–172.

Shariati, A., Peters, C.J., 2003. Recent developments in particle design using supercritical fluids. Curr. Opin. Solid State Mater. Sci. 7, 371–383.

Subramaniam, B., Rajewski, R.A., Snavely, K., 1997. Pharmaceutical processing with supercritical carbon dioxide. J. Pharm. Sci. 86, 885–890.

Titulaer, H.A.C., Zuidema, J., Lugt, C.B., 1991. Formulation and pharmacokinetics of arthemisinin and its derivatives. Int. J. Pharm. 69, 83–92.

Wong, J.W., Yuen, K.H., 2001. Improved oral bioavailability of artemisinin through inclusion complexation with β-, and γ- cyclodextrins. Int. J. Pharm. 227, 177–185.

Wong, J.W., Yuen, K.H., 2003. Inclusion complexation of artemisinin with α-,β-, and γ- cyclodextrins. Drug Dev. Ind. Pharm. 29, 1035–1044.

Yalkowsky, S.H. (Ed.), 1981. Techniques of Solubilization of Drugs. Marcel Dekker, NY.

Zhao, S.S., 1987. High-performance liquid chromatographic determination of artemisinin (qinghaosu) in human plasma and saliva. Analyst 112, 661–664.